energies

MDPI

Article

A Discrete Electrical Model for Photovoltaic Solar Cells—d1MxP

João Paulo N. Torres [1,2], Ricardo A. Marques Lameirinhas [2,3,*], Catarina P. Correia V. Bernardo [3], Helena Isabel Veiga [1] and Pedro Mendonça dos Santos [1,2]

[1] Academia Militar/CINAMIL, Av. Conde Castro Guimarães, 2720-113 Amadora, Portugal
[2] Instituto de Telecomunicações, 1049-001 Lisbon, Portugal
[3] Department of Electrical and Computer Engineering, Instituto Superior Técnico, 1049-001 Lisbon, Portugal
* Correspondence: ricardo.lameirinhas@tecnico.ulisboa.pt

Abstract: Solar cell equivalent circuit modelling is usually based on continuous I-V models, with a set of data obtained by analytical expressions. This work proposes an almost discrete novel mathematical method and correspondent electrical model, based on the I-V curve adjustment at every two adjacent points. It is based on the discretisation of any diode model behaviour, such as the 1M5P (also known as 1D5P) or the 1M7P (also known as 2D7P). For this reason, the model is named d1MxP, meaning that it is a discrete (d) model (1M) with x parameters (xP). The modelling methodology validation process uses experimental data already published in the literature. According to the presented results, the proposed method shows increased accuracy when compared to the 1M5P or 1M7P equivalent models. The accuracy on the maximum power point and fill factor determination is relevant, resulting in an improvement of up to 3.34% in the maximum power, up to 5.70% in its voltage and up to 8.20% in its current, for the analysed data. Furthermore, Fill Factor values, have variation from up to 35.98%. The temperature influence on the silicon solar cell is also analysed, to validate the results. The proposed method allows highly accurate curve fitting to the (experimental) points and consequently, to obtain a more accurate model to analyse the performance of solar cells under different conditions.

Keywords: 1M5P; d1MxP; photovoltaic technology; solar cell; solar cell equivalent model; solar energy

Citation: Torres, J.P.N.; Marques Lameirinhas, R.A.; Correia V. Bernardo, C.P.; Veiga, H.I.; dos Santos, P.M. A Discrete Electrical Model for Photovoltaic Solar Cells—d1MxP. *Energies* **2023**, *16*, 2018. https://doi.org/10.3390/en16042018

Academic Editor: Alon Kuperman

Received: 26 January 2023
Revised: 12 February 2023
Accepted: 14 February 2023
Published: 17 February 2023

1. Introduction

Due to the unlimited use of the Earth's natural resources, the increase in the concentration of greenhouse gases and the rise in average global temperatures has led to the urgent need for cleaner and renewable energy sources [1–4]. In recent years, solar energy has reached installation record values and it is considered one of the most important renewable energy sources. This type of green energy also contributes to the economic development of a more wide group of countries. Although the initial investment might be huge, natural resources are available around the world, being a never-ending source of energy. In the case of solar radiation that reaches the Earth's surface, electricity is generated through the photoelectric effect/conversion, leading to comparative advantages in cost, technological setup complexity and environmental benefits [1,5].

In the last decades, the development of solar cells evolved in three technological generations, mainly due to the use of different materials and architectures [1,6,7]. Solar cells based on crystalline silicon structures are widely used and have high efficiencies. These types of cells are dominating the technology market, since silicon is an abundant element on Earth, with a non-toxic manufacturing process [1,7–10].

As with many other semiconductor devices, the solar cell can be included and simulated in circuit analyses with the aid of an electrical model, which represents its electrical performance and working principle [1,8]. Generally, those models are based on continuous I-V functions, which can be obtained from a mathematical fitting of a set of experimental data. This fitting preserves a certain I-V shape, which is considered from the solar cell ideal

working principle. The electrical model can be almost ideal, such as the 1M3P (one Model of three Parameters), which only takes into account the p-n junction diode characteristic at dark mode, or can be made more accurate, including resistive losses, such as those depicted in 1M5P (one Model of five Parameters) [1,11].

The motivation to proposed this model is based on the graphical connections between consecutive I-V points. When one is analysing the points in any tool as a continuous plot, the tool just connect the scatter points. The aim of this research work is to try to develop a model based on the 1M5P and on that fact: connecting adjacent points (with small voltage difference) must be better than obtaining a certain number of parameters that represents the whole voltage range (as the continuous models do). It is done by discretizing the diode on the 1M5P (or 1MxP in general), and for that reason, the proposed model is named as d1MxP, meaning that it is a discrete (d) model (1M) with x parameters (xP). The discretization is done using the equivalent model of a diode, which is a series of an ideal diode, a resistance and an independent voltage source.

2. Methodology

The solar cell electrical model is an approach to characterise the major physical phenomena and working principles that occur in the device [1].

The model proposed in this work is based on the discrete analyses of the well-known 1M5P model, illustrated in Figure 1, but the discretization can also be applied to more complex models, with an increased number o diode brunches, such as the 1M7P (also known as 2D7P) model [1,12]. For that reason, the proposed model will be hereafter named d1MxP (d for discrete, with x parameters).

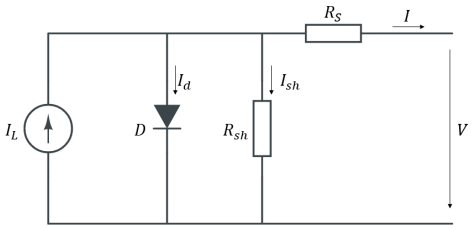

Figure 1. The 1M5P equivalent circuit model of a photovoltaic solar cell.

Based on simple circuit analyses and on the p-n junction working principle, it is possible to analytically define the current-voltage (I-V) characteristic of a solar cell through the Equation (1). Referring again to Figure 1, I_L is the photogenerated current, I_d is the current that passes through the diode, I_o is the diode reverse current (also known as the diode saturation current) and I_{sh} is the current that passes through the shunt resistance. In Equation (1), V_T is the thermal voltage, which is given by Equation (2) (usually assumed at room temperature, leading to a value of 26 mV), where k is the Boltzmann's constant, T is the temperature and q is the electron charge, n is the diode non-ideality factor, R_s is the series resistance associated to a voltage loss due to the cell's connections and R_{sh} is the shunt/parallel resistance related to a current loss due to current leaks on the cell [1,13,14].

$$I = I_L - I_d - I_{sh} = I_L - I_o\left(e^{\frac{V+R_sI}{nV_T}} - 1\right) - \frac{V + R_sI}{R_{sh}} \quad (1)$$

$$V_T = \frac{kT}{q}. \quad (2)$$

The first difficulty in using this model is that the independent variable, the cell's output current, depends not only on the cell's output voltage but also on itself (cell's output current), leading to an implicit mathematical function. In this scenario, the Newton–Raphson algorithm is applied as depicted in Equation (3), where $f(I)$ corresponds to the function

that translates the current-voltage relation of a solar cell, Equation (1), and $f'(I)$ is its first derivative, with respect to I (current function's derivative with respect to the current). For each V, the output current I is determined based on the Newton–Raphson algorithm, given by Equation (3), where i is the iteration index.

$$I_{i+1} = I_i - \frac{f(I)}{f'(I)}. \tag{3}$$

Equations (4) and (5) were used to extract the five model parameters: R_s, R_{sh}, I_o, n and I_L. This methodology is based on a set of relevant experimental points, namely, the short-circuit current I_{SC}, and the open-circuit voltage V_{OC}. To obtain the value for n based on expression (5) it is necessary to perform graphical or iterative techniques [14]. For example, the 1M3P model is obtained when $R_s = 0\ \Omega$ and $R_{sh} = \infty\ \Omega$ [1,14]. V_{mp} and I_{mp} in Equation (5) correspond to the I-V coordinates of the point of maximum power, which is the point where the solar cell is delivering the maximum power for a specific load [1].

$$\begin{cases} R_s = -\dfrac{1}{\frac{dI}{dV}|_{V=V_{OC}}} \\ R_{sh} = -\dfrac{1}{\frac{dI}{dV}|_{I=I_{SC}}} \\ I_o = \dfrac{I_{SC}\left(1+\frac{R_s}{R_{sh}}\right) - \frac{V_{OC}}{R_{sh}}}{e^{\frac{V_{OC}}{nV_T}}} \\ I_L = I_o\left(e^{\frac{V_{OC}}{nV_T}} - 1\right) + \dfrac{V_{OC}}{R_{sh}} \end{cases} \tag{4}$$

$$\begin{aligned} n \to ln\left(I_{SC}\left(1+\frac{R_s}{R_{sh}}\right) - \frac{V_{mp}}{R_{sh}} - I_{mp}\left(1+\frac{R_s}{R_{sh}}\right)\right) = \\ ln\left(I_{SC}\left(1+\frac{R_s}{R_{sh}}\right) - \frac{V_{OC}}{R_{sh}}\right) - \frac{V_{OC}}{nV_T} + \frac{V_{mp}+R_s I_{mp}}{nV_T}. \end{aligned} \tag{5}$$

The main disadvantage of this classic approach is that the entire voltage range is characterised by the same equation, which is prone to local inaccuracies. Even worse, when the model is deeply analysed and the five parameters are obtained with expressions (4) and (5), it is possible to verify that only a few number of points are used for fitting in the whole range. In fact, R_s is only dependent on a small number of points near the open-circuit voltage (sometimes only two since it is the simplest way to compute the curve slope). The same happens for the R_{sh} parasitic resistance, but near the short-circuit current path of the I-V experimental data. The photogenerated current is just one single point, at most an average of a few points near the current axis and the I_0 and n are obtained using points on the curve slope (typically two, as suggested).

The model proposed in this work considers the solar cell performance between two adjacent (experimental) points, which is equivalent to an analytical incremental calculation. In this way, the solar cell diode is decomposed into a set of adjustable parallel diodes, to attain an increased overall precision in the considered solar cell voltage range. Figure 2 presents an equivalent model of the diode in the solar cell model. The subset model is composed of an ideal diode (an ideal electrical switch, which might be characterised as a diode with null voltage drop at on-state, null on-state resistance, infinite breakdown/reverse voltage and without parasitic capacitive effects), in series with a given resistance and an ideal independent voltage source. Figure 3 represents the I-V curve obtained from this equivalent model. The ideal diode has its characteristic in red and the curve of the entire serial branch is in light blue. The diode is at on-state (as an ideal closed switch) whenever its anode voltage is above the voltage source Vγ. With the ideal diode at on-state, the branch collects current from the model current source, leading to less available current

at the cell terminals. The slope of the I-V curve with this diode equivalent model is then proportional to $-1/R_\gamma$.

Based on this approach, it is possible to extend the concept in order to connect two adjacent points in the I-V curve obtained experimentally, as suggested in Figure 4. As can be seen, the slope between these two adjacent points is dependent on the resistance of the branch. On the other hand, with a specific sizing methodology, the ideal diode at branch N can become responsible to activate the respective branch, considering the effect of the entire N-1 parallel branches previously activated. The N branch resistance is only associated with the angle to adjust the previous slope to the next one, meaning that the resistance value is based on the previous and on the pretended slope, m. The resultant calculation process is equivalent to adding weighted resistances in parallel to attain a curve fitting to the experimental data. The mathematical formalism is presented in the system of Equation (6) and Figure 5 is the illustration of the obtained equivalent circuit model for N branches.

$$\begin{cases} V_\gamma = V_i \\ R_\gamma = -\dfrac{1 + m_i m_{i-1}}{m_i - m_{i-1}}. \end{cases} \tag{6}$$

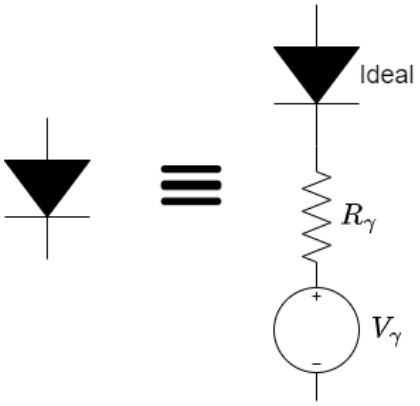

Figure 2. Diode equivalent model.

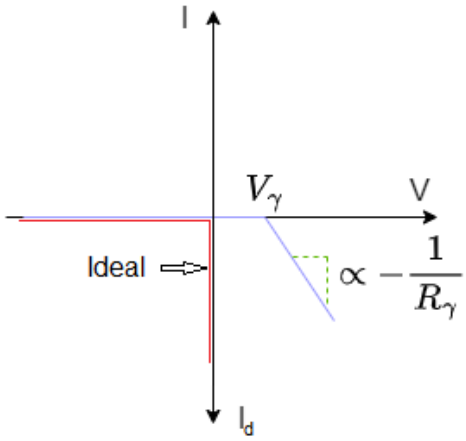

Figure 3. I-V curves obtained from the ideal (red) and non-ideal (light blue) diode equivalent model.

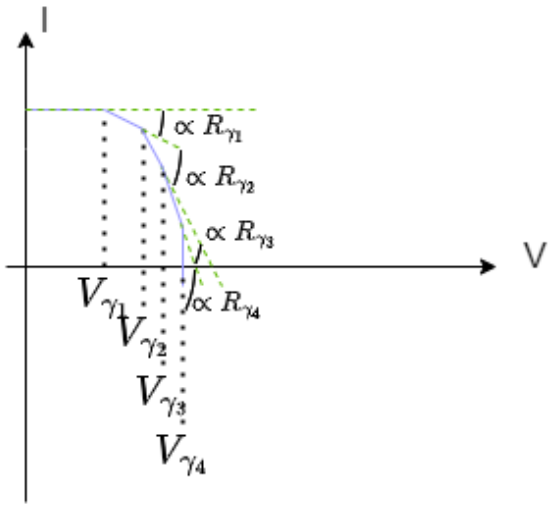

Figure 4. I-V curve for N branches in parallel (N = 4, as an example).

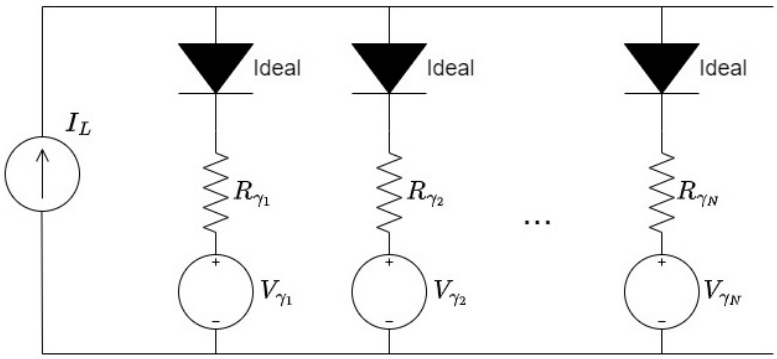

Figure 5. Proposed equivalent circuit model of a photovoltaic solar cell: d1MxP.

Shunt and series resistances are not explicitly represented in the model. However, the shunt resistance (current losses) is the one associated with a null-voltage, meaning that the branch is active in the whole range reducing the current flow from the current source to the load (output). On the other hand, the series resistance is not directly computed in the model, but the voltage losses (the meaning of that resistance in 1M5P model) are associated to the slope variation near the solar cell open-circuit characteristic.

Since this model is based on 1MxP/1DxP (1M7P or 1M5P for instance), some assumptions are made. The assumptions are the same to the ones performed on the application of these models. The most important to be highlighted is that these models assume that the I-V slope decreases (becomes more negative) by increasing the output resistive load (or voltage). The exponential behaviour of the diode I-V curve leads to the increase of the slope's magnitude by increasing the voltage. This assumption comes from the assumptions of 1M5P or 1M7P models [1,15–17]. Experimentally, it is possible to obtain sequences of points that do not follow this rule. In these cases, the model considers these points as outliers. Since the experimental I-V curve data usually have a very low quantity of outliers, it is expected that the proposed model should continue to follow the experimental behaviour.

3. Model Evaluation and Validation

The cell temperature has a significant impact on the behaviour of the I-V and P-V characteristic curves [1,3,15–20]. In order to evaluate the model under study, taking into account the significant impact of temperature, several tests at different temperatures were analysed. Due to its matured scientific phenomena knowledge, the model evaluation and validation is based on mono-crystalline silicon cells technology.

3.1. I-V and P-V Curves from d1MxP and 1M5P Models

In order to validate the proposed methodology, experimental data obtained from the literature were used. The iterative proposed model was implemented in MATLAB. The experimental I-V points obtained from [19] were measured on a mono-Si solar cell, at a constant light intensity of 550 W/m^2 and at different temperatures.

Figure 6 shows the 25 points obtained from [19] at 25 °C. Based on the 1M5P set of equations presented above, it is possible to obtain $I_L = 0.226$ A, $I_o = 7.270 \times 10^{-18}$ A, $n = 0.572$, $R_{sh} = 90.319\ \Omega$ and R_s =0.391 Ω. The correspondent I-V curve is also presented in the figure (yellow line). The red curve is the I-V curve computed using the proposed novel methodology. As can be confirmed, this curve is in good agreement with the experimental points, significantly reducing the error obtained from the 1M5P model in all the voltage range. Table 1 summarises the d1MxP model parameters for each branch. Using these experimental data, the model has 12 branches and 24 parameters (d1M24P). As expected, the higher the slope variation, the lower the branch resistance. As mentioned before, shunt and series resistances are not explicit in the model. However, the shunt resistance (current losses) is the one in the first branch since it is associated to a null-voltage, meaning the branch is active in the whole range reducing the current flow from the current source to the load (output). This statement is corroborated by comparing both values (89.217 Ω on d1MxP and $R_{sh} = 90.319\ \Omega$ on 1M5P). On the other hand, the series resistance is not directly computed in the model, but the voltage losses (the meaning of this resistance in 1M5P model) are associated to the slope variation near the open-circuit that is quite well-characterised using the proposed model.

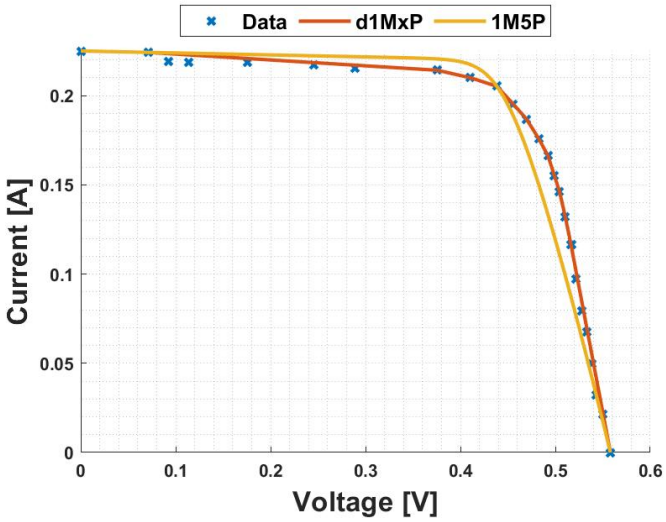

Figure 6. I-V curves using the 1M5P model and the proposed model, at T = 25 °C.

Table 1. Quantitative values computed for the branches connected in parallel, for T = 25 °C.

N	R_γ [Ω]	V_γ [V]
1	89.217	0
2	46.209	0.071
3	11.384	0.376
4	20.753	0.410
5	2.712	0.438
6	44.543	0.456
7	6.249	0.470
8	12.856	0.483
9	4.027	0.492
10	6.990	0.504
11	27.201	0.510
12	39.350	0.517

The P-V characteristics at 25 °C are presented in Figure 7 for the proposed d1MxP model, in comparison with the P-V curve obtained with the 1M5P models. As can be confirmed, the curve for the proposed model (in red) presents a more precise fitting to the experimental data, which results in a more accurate quantification of the maximum power point.

The I-V characteristics of the solar cell at 40 °C are illustrated in Figure 8, for the same load condition. At this temperature, the five parameters of the 1M5P model were computed as $I_L = 0.237$ A, $I_o = 3.105 \times 10^{-20}$ A , $n = 0.461$, $R_{sh} = 47.583$ Ω and $R_s = 0.403$ Ω, resulting in a curve similar to the one obtained for 25 °C. The parameters computed to obtain the d1MxP curve are summarised in Table 2 (in this case $x = 30$). As before, the curve shape keeps tracking the experimental data with more accuracy than the classical 1M5P model.

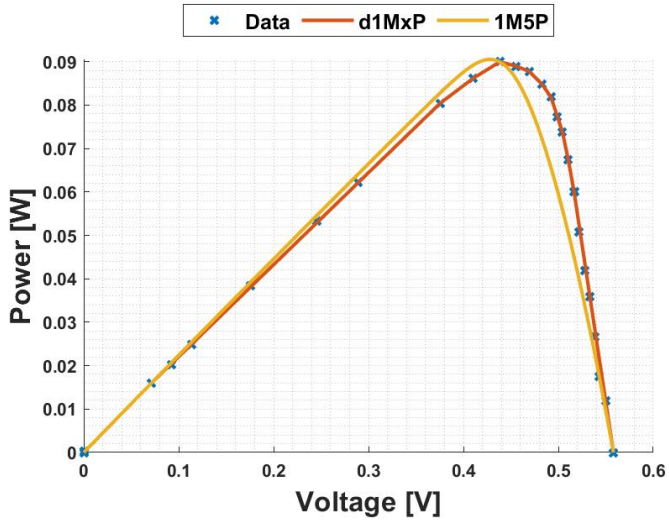

Figure 7. P-V curves using the 1M5P model and the proposed model, at T = 25 °C.

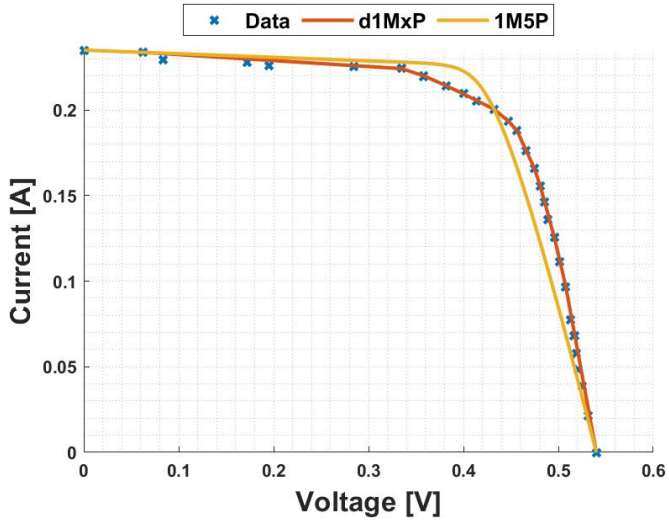

Figure 8. I-V curves using the 1M5P model and the proposed model, at T = 40 °C.

The P-V curves for 40 °C are shown in Figure 9. The difference between the d1M5xP and the 1M5P model characteristics is now more noticeable at this temperature. As expected, the proposed d1MxP model follows the experimental data with more accuracy, especially at the maximum power point.

Table 2. Quantitative values computed for the branches connected in parallel, for T = 40 °C.

N	R_γ [Ω]	V_γ [V]
1	46.922	0
2	74.154	0.063
3	6.962	0.335
4	15.527	0.358
5	83.059	0.382
6	57.348	0.400
7	6.109	0.432
8	8.989	0.447
9	2.863	0.457
10	8.541×10^{14}	0.466
11	6.913	0.475
12	11.212	0.481
13	18.802	0.496
14	76.934	0.502
15	14.072	0.508

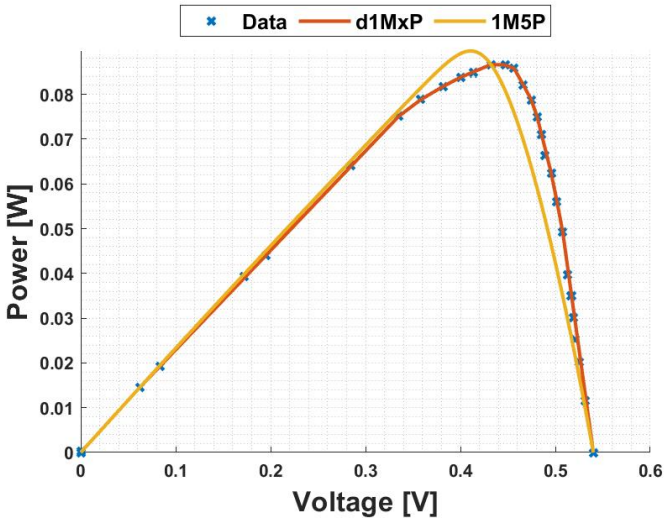

Figure 9. P-V curves using the 1M5P model and the proposed model, at T = 40 °C.

At 50 °C, the 1M5P parameters are $I_L = 0.243$ A, $I_o = 7.576 \times 10^{-21}$ A, $n = 0.423$, $R_{sh} = 34.696$ Ω and $R_s = 0.422$ Ω, and the curves are illustrated in Figure 10. This figure also includes the experimental data and the d1M5xP curve (in this case $x = 24$). The parameters of d1MxP are in Table 3 and the P-V comparative curves are shown in Figure 11.

Table 3. Quantitative values computed for the branches connected in parallel, for T = 50 °C.

N	R_γ [Ω]	V_γ [V]
1	34.145	0
2	66.247	0.055
3	22.506	0.280
4	22.244	0.369
5	4.244	0.392
6	6.534	0.409
7	4.813	0.437
8	6.831	0.447
9	14.223	0.463
10	5.216	0.470
11	11.058	0.487
12	20.481	0.503

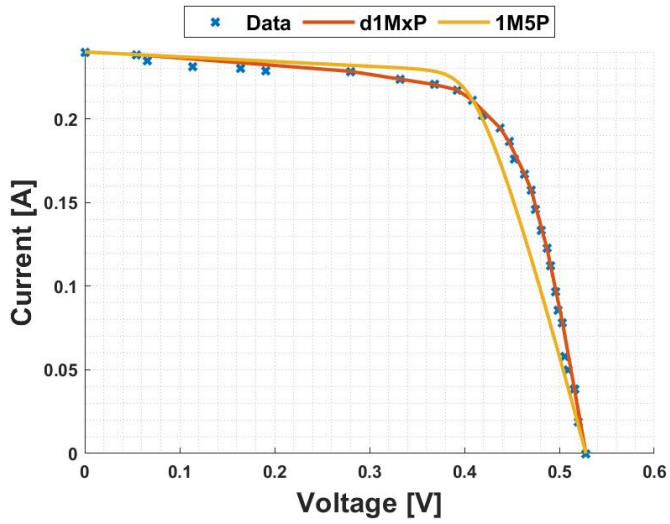

Figure 10. I-V curves using the 1M5P model and the proposed model, at T = 50 °C.

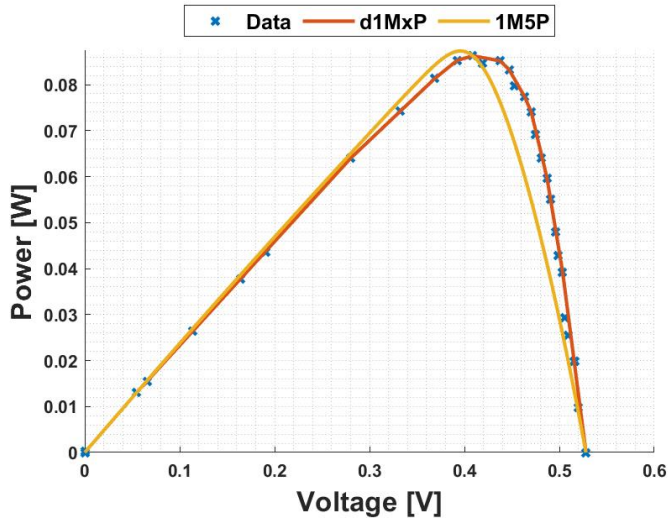

Figure 11. P-V curves using the 1M5P model and the proposed model, at T = 50 °C.

The last temperature is 60 °C and the I-V curves of both models are presented in Figure 12. The 1M5P computed parameters were $I_L = 0.248$ A, $I_o = 1.067 \times 10^{-13}$ A, $n = 0.631$, $R_{sh} = 35.687\ \Omega$ and $R_s = 0.424\ \Omega$ and the parameters for the d1MxP are shown in Table 4. As expected, the d1MxP ($x = 18$) model fitting is more accurate than the 1M5P curve. The P-V curves are in Figure 13 corroborating the previous conclusions.

Table 4. Quantitative values computed for the branches connected in parallel, for T = 60 °C.

N	R_γ [Ω]	V_γ [V]
1	35.026	0
2	32.910	0.047
3	10.928	0.252
4	9.728	0.332
5	4.390	0.391
6	10.680	0.421
7	2.819	0.436
8	4.830	0.463
9	5.982	0.486

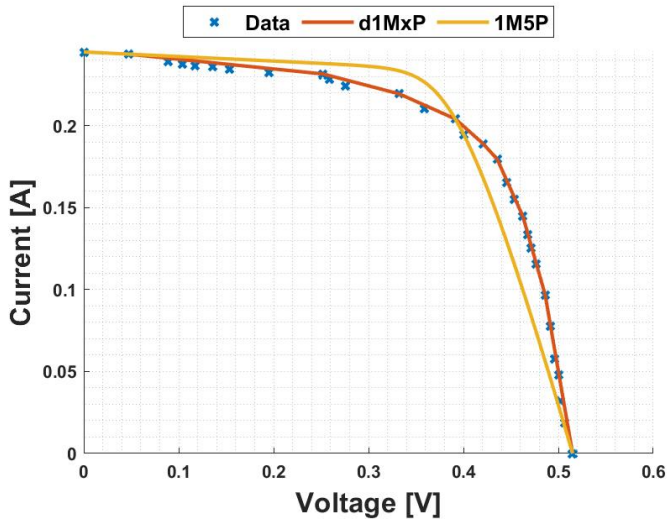

Figure 12. I-V curves using the 1M5P model and the proposed model, at T = 60 °C.

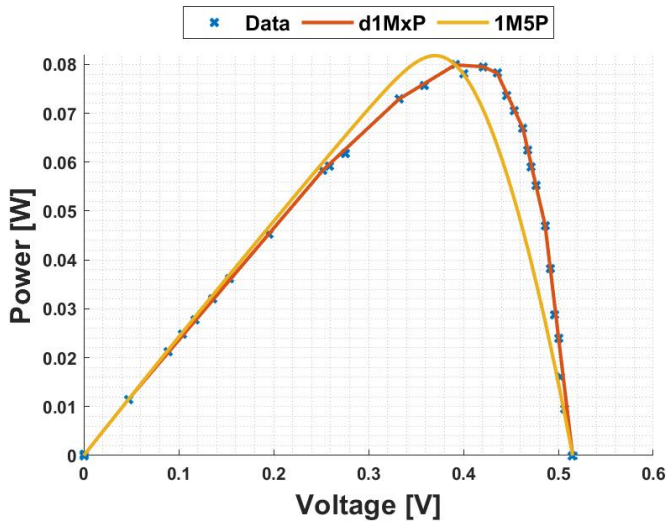

Figure 13. P-V curves using the 1M5P model and the proposed model, at T = 60 °C.

3.2. Results Analysis

Table 5 summarises the comparative maximum power points (power, voltage and current) for the evaluated temperatures, together with the difference between the proposed model and the classical 1M5P model as a reference. It is possible to verify that there are significant differences between models. Additionally, according to the evaluation based on the I-V and P-V curves for different temperatures, it is obvious that the proposed method is more accurate. In fact, the proposed model allows a correction of approximately 0.55% to 3.34% in the maximum power value, of 2.38% to 5.70% in the voltage value of the maximum power point and of 2.93% to 8.20% in its current.

Table 6 presents the Fill Factor values for the proposed model and compares it with the experimental Fill Factor recorded in the literature [19]. As can be seen, the d1MxP model leads to an increase in the Fill Factor, due to the more accurate fit to the experimental data. The literature Fill Factor is determined using the 1M3P formula [19] instead of the 1M5P one, meaning that the curve is treated as a rectangle. Consequently, this factor constitutes an advantage of the proposed model, since the Fill Factor is obtained using the trapezoids below the computed points.

Table 5. Maximum power (P_{max}), maximum voltage (V_{max}) and maximum current (I_{max}) values obtained with the proposed and the 1M5P models.

		d1MxP	1M5P	Δ (%)
T = 25 °C	P_{max} [W]	0.0900	0.0905	0.55
	V_{max} [V]	0.4383	0.4281	2.38
	I_{max} [A]	0.2053	0.2115	2.93
T = 40 °C	P_{max} [W]	0.0867	0.0897	3.35
	V_{max} [V]	0.4322	0.4107	5.24
	I_{max} [A]	0.2005	0.2184	8.20
T = 50 °C	P_{max} [W]	0.0863	0.0873	1.15
	V_{max} [V]	0.4087	0.3958	3.26
	I_{max} [A]	0.2111	0.2206	4.31
T = 60 °C	P_{max} [W]	0.0799	0.0818	2.32
	V_{max} [V]	0.3913	0.3702	5.70
	I_{max} [A]	0.2042	0.2209	7.56

Table 6. Fill Factor values obtained using different methodologies.

	Data (Ref. [19])	d1MxP	Δ (%)
T = 25 °C	0.7044	0.8917	26.59
T = 40 °C	0.6900	0.8803	27.58
T = 50 °C	0.6644	0.8750	31.70
T = 60 °C	0.6292	0.8556	35.98

The computed Fill Factor values show a variation from 26.59% to 35.98%, when compared with the data reported in [19]. These values are higher than those presented for the maximum power point, since the FF was computed using the area above the d1MxP curves, which is the area above the experimental data (at least the computed points).

Figures 14 and 15 show the behaviour of the d1MxP model for the different temperatures under evaluation. The proposed d1MxP model tracks the significant and well-known impact that temperature causes on the behaviour of the solar cell characteristic curve. As can be seen, the increase in temperature leads to a decrease in the maximum power achieved by the solar cell. Fill Factor also decreases by increasing the temperature. As predicted, the open-circuit voltage decreases with temperature, while the short-circuit current increases [1].

The temperature variation does not change the I-V and P-V curves' shapes of the silicon solar cell. The I-V curves cross among them near the maximum power point, since the short-circuit current increases and the open-circuit voltage decreases by increasing the temperature. The P-V maximum point (maximum power point) moves in diagonal (the output power is the multiplication of both axis quantities), keeping the curve shape, as expected.

The presented results suggest that d1MxP model might be used to characterise other more complex solar cells or the effect of complex phenomena on their performance. In these cases, the I-V curves might have different shapes from the one imposed on the 1M5P model. For that reason, in comparison with 1M5P, the proposed model should fit better on them.

Also, the variation of the branch resistances of d1MxP model might be studied if the analysed loads (load resistances or output voltages) are the same among different tests/conditions. Thus, one should find a certain mathematical function of values pattern to characterise the variation of branch resistances with a certain condition, such as temperature.

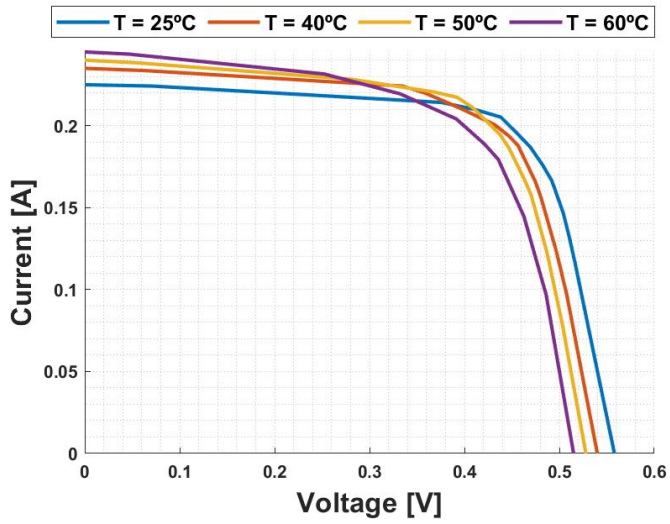

Figure 14. Summary of the I-V curves obtained with the d1MxP model for different temperatures.

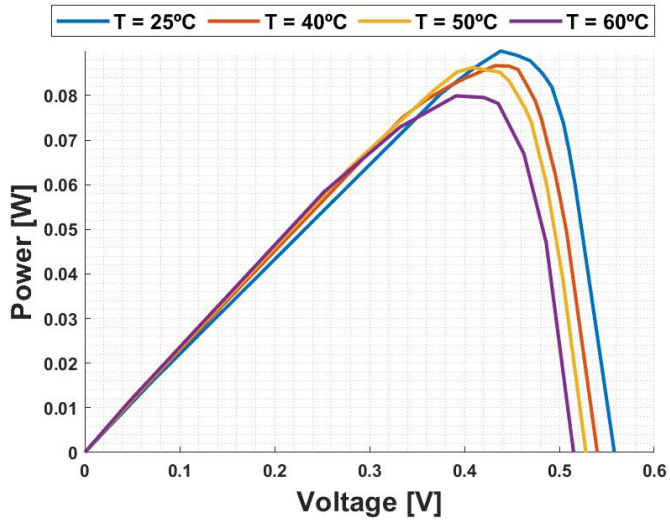

Figure 15. Summary of the P-V curves obtained with the d1MxP model for different temperatures.

4. Conclusions

The aim of this research work is to evaluate and validate a more accurate electrical model for characterising solar cells' performance. Aiming the error minimisation, the proposed electrical model tries to connect every two adjacent points of a I-V curve, in contrast to the classic 1M5P model (or, in general, 1MxP models), which uses a small portion of the data set to characterise the entire voltage range.

The proposed model uses a subset of parallel and finite branches based on the 1M5P diode model, discretizing the diode electrical performance and using its own equivalent model. Thus, its exponential I-V curve is section-wise linear in the model, which is quite useful for characterising the performance of a set of solar cells. All the imperfections in a solar cell might be better characterised using this approach.

The proposed mathematical and electrical model allows us to follow experimental data and the computation of more accurate I-V and P-V curves. Consequently, the estimation of the maximum power point, the Fill Factor, efficiency and other figures of merit can become more accurate and precise, when compared with the 1M5P or 1M7P equivalent models. In this case, it results in an improvement of up to 3.34% in the maximum power, up to 5.70% in its voltage and up to 8.20% in its current. On the other hand, a variation up to 35.98% was registered in the Fill Factor determination.

Author Contributions: Conceptualization: R.A.M.L., C.P.C.V.B. and J.P.N.T.; Methodology: R.A.M.L. and C.P.C.V.B.; Software: R.A.M.L. and C.P.C.V.B.; Investigation: R.A.M.L., C.P.C.V.B., J.P.N.T., H.I.V. and P.M.d.S.; Writing—original draft: R.A.M.L. and C.P.C.V.B.; Writing—review & editing: R.A.M.L. and P.M.d.S. All authors have read and agreed to the published version of the manuscript.

Funding: This research received no external funding.

Institutional Review Board Statement: Not applicable.

Informed Consent Statement: Not applicable.

Data Availability Statement: Not applicable.

Acknowledgments: This work was supported in part by FCT/MCTES through national funds and in part by cofounded EU funds under Project UIDB/50008/2020. This work was also supported by FCT under the research grant UI/BD/151091/2021.

Conflicts of Interest: The authors declare no conflict of interest.

References

1. Marques Lameirinhas, R.A.; Torres, J.P.N.; de Melo Cunha, J.P. A Photovoltaic Technology Review: History, Fundamentals and Applications. *Energies* **2022**, *15*, 1823. [CrossRef]
2. El Chaar, L.; Lamont, L.A.; El Zein, N. Review of photovoltaic technologies. *Renew. Sustain. Energy Rev.* **2011**, *15*, 2165–2175. [CrossRef]
3. Zaini, N.H.; Ab Kadir, M. Z.; Izadi, M.; Ahmad, N.I.; Radzi, M.A.M.; Azis, N. The effect of temperature on a mono-crystalline solar PV panel. In Proceedings of the 2015 IEEE Conference on Energy Conversion (CENCON), Johor Bahru, Malaysia, 19–20 October 2015. [CrossRef]
4. Antunes Alves dos Santos, S.; Torres, J.P.N.; Fernandes, C.A.F.; Marques Lameirinhas, R.A. The impact of aging of solar cells on the performance of photovoltaic panels. *Energy Convers. Manag. X* **2021**, *10*, 100082. [CrossRef]
5. Sinke, W.C. Development of photovoltaic technologies for global impact. *Renew. Energy* **2019**, *138*, 911–914. [CrossRef]
6. Asdrubali, F.; Desideri, U. Chapter 7—High Efficiency Plants and Building Integrated Renewable Energy Systems. In *Handbook of Energy Efficiency in Buildings*; Elsevier: Amsterdam, The Netherlands, 2019. [CrossRef]
7. Pinho Correia Valério Bernardo, C., Marques Lameirinhas, R.A., Neto Torres, J.P.; Baptista, A. Comparative analysis between traditional and emerging technologies: Economic and viability evaluation in a real case scenario. *Mater. Renew. Sustain. Energy* **2023**. [CrossRef]
8. Alves, T.; N. Torres, J.P.; Marques Lameirinhas, R.A.; F. Fernandes, C.A. Different Techniques to Mitigate Partial Shading in Photovoltaic Panels. *Energies* **2021**, *14*, 3863. [CrossRef]
9. De Melo Cunha, J.P.; Marques Lameirinhas, R.A.; N. Torres, J.P. Multi-Junction Solar Cells and Nanoantennas. *Nanomaterials* **2022**, *12*, 3173. [CrossRef] [PubMed]
10. Green, M.A. Silicon photovoltaic modules: A brief history of the first 50 years. *Prog. Photovoltaics Res. Appl.* **2005**, *13*, 447–455. [CrossRef]
11. Rui, C.; Silva, M. Experimental and Theoretical Validation of One Diode and Three Parameters–Based PV Models. *Energies* **2021**, *14*, 2140. [CrossRef]
12. Yuqiang, L.; Li, Y.; Wu, Y.; Yang, G.; Mazzarella, L.; Procel-Moya, P.; Tamboli, A.C.; Weber, K.; Boccard, M.; Isabella, O.; et al. High-Efficiency Silicon Heterojunction Solar Cells: Materials, Devices and Applications. *Mater. Sci. Eng. Rep.* **2020**, *147*, 100579.
13. Firoz K.; Singh, S.N.; Husain, M. Effect of illumination intensity on cell parameters of a silicon solar cell. *Sol. Energy Mater. Sol. Cells* **2010**, *94*, 1473–1476. [CrossRef]
14. Zhaoxu, S.; Kun, F.; Xiaofang, S.; Ying, L.; Wei, L.; Chuanzhong, X.; Gongyi, H.; Fei, Y. An Effective Method to Accurately Extract the Parameters of Single Diode Model of Solar Cells. *Nanomaterials* **2021**, *11*, 2615. [CrossRef]
15. Skoplaki, E.; Palyvos, J.A. On the temperature dependence of photovoltaic module electrical performance: A review of efficiency/power correlations. *Solar Energy* **2009**, *83*, 614–624. [CrossRef]
16. Babu, B.C.; Gurjar, S. A Novel Simplified Two-Diode Model of Photovoltaic (PV) Module. *IEEE J. Photovoltaics* **2014**, *4*, 1156–1161. [CrossRef]
17. Ortiz-Conde, A.; Lugo-Muñoz, D.; García-Sánchez, F. J. An Explicit Multiexponential Model as an Alternative to Traditional Solar Cell Models With Series and Shunt Resistances. *IEEE J. Photovoltaics* **2012**, *2*, 61–268. [CrossRef]
18. De Oliveira Santos, L.; de Carvalho, P.C.M.; de Oliveira Carvalho Filho, C. Photovoltaic Cell Operating Temperature Models: A Review of Correlations and Parameters. *IEEE J. Photovoltaics* **2022**, *12*, 179–190. [CrossRef]

19. Subhash, C.; Purohit, A.; Sharma, A.; Nehra, S.P.; Dhaka, M.S. Impact of temperature on performance of series and parallel connected mono-crystalline silicon solar cells. *Energy Rep.* **2015**, *1*, 175–180. [CrossRef]
20. Singh, P.; Ravindra, N.M. Temperature dependence of solar cell performance—An analysis. *Sol. Energy Mater. Sol. Cells* **2012**, *101*, 36–45. [CrossRef]